

Metallicity and disorder at the alkali-metal/GaAs(001) interface

O. E. Tereshchenko

*Laboratoire de Physique de la Matière Condensée, Ecole Polytechnique, 91128 Palaiseau Cedex, France
and Institute of Semiconductor Physics, 630090 Novosibirsk, Russia*

D. V. Daineka

*Laboratoire de Physique de la Matière Condensée, Ecole Polytechnique, 91128 Palaiseau Cedex, France
and A. F. Ioffe Physico-Technical Institute, 194021 St. Petersburg, Russia*

D. Paget

Laboratoire de Physique de la Matière Condensée, Ecole Polytechnique, 91128 Palaiseau Cedex, France

(Received 20 November 2000; revised manuscript received 18 April 2001; published 7 August 2001)

We have investigated the adsorption of sodium and potassium on GaAs(001) at temperatures ranging between 85 K and 300 K. Photoreflectance spectroscopy and electron-energy-loss spectroscopy are used to characterize the formation of a metallic phase through, respectively, the photovoltage value and the presence of surface plasmons in the loss spectrum. Reflectance-anisotropy spectroscopy allows us to characterize the disorder of the adsorbate as found from the width of the line at 2.3 eV, which characterizes the spectrum of the gallium-rich surface. If the alkali-metal adsorption is performed at a temperature lower than 200 K, there occurs a nonmetal-metal transition at a submonolayer coverage. The metallic phase appears abruptly near 0.4–0.5 ML, and there exists a transition regime where both metallic and nonmetallic phases coexist. Subsequent adsorption leads to the abrupt disappearance of the nonmetallic phase. At low temperature, the adsorbate is found to be disordered since surface diffusion of sodium and to some extent of potassium is prohibited. The metallic phase is metastable and irreversibly disappears under annealing to RT, at a temperature at which surface diffusion becomes thermally allowed. As a result, the presence of metallicity is directly related to the disorder of the adsorbate. For Na and for K, we have determined the diagram of existence of the disordered metallic phase as a function of temperature and coverage, as well as of the transition region.

DOI: 10.1103/PhysRevB.64.085310

PACS number(s): 78.66.Fd, 73.50.Pz, 73.20.Mf, 73.40.Ns

I. INTRODUCTION

Adsorption of alkali metals (AM's) on various substrates has been widely investigated because of the simplicity of the interface formation and because of its technological interest. Such adsorption has been investigated in detail in the case of metallic substrates^{1–4} and gives rise to a wealth of regimes, which have been described under the form of phase diagrams as a function of coverage and temperature. At low coverage, the interaction between the adsorbate atoms is negligible so that the atoms occupy preferential adsorption sites determined by the substrate. If the coverage is increased, there occurs a competition between the adatom-substrate interaction and the adatom-adatom interaction, in which several distinct phases can be observed. These phases can be ordered or disordered, and commensurate or incommensurate with the substrate. At a larger coverage, the stronger adatom-adatom interaction favors the formation of incommensurate phases, in which the adsorbate structure is less dependent on the substrate. The effect of temperature is important for the structure of the adsorbate, since it has been found⁵ that at low temperature surface diffusion is prohibited so that the adsorbate is relatively disordered, whereas upon increasing the temperature surface diffusion becomes allowed, which leads to a disorder-order phase transition.

AM adsorption on semiconducting substrates has also been intensively investigated in order to analyze the effect of the substrate on the geometrical and electronic properties of

the adsorbate. For the cleavage face of GaAs, several ordered phases have been observed at submonolayer coverages using scanning-tunneling microscopy (STM).⁶ These phases are insulating, which has been explained as due to electron-correlation effects so that at RT the system behaves as a Mott insulator.⁷ For RT adsorption on silicon, the adsorption sites of several alkali atoms and the metallicity of the surface have been investigated using STM,⁸ photoemission,⁹ electron-energy-loss spectroscopy (EELS),¹⁰ and x-ray diffraction.¹¹

In comparison with the above works, only a small number of studies have considered the effect of adsorption temperature on the structure and electronic properties of the adsorbate.^{12–17} Such an effect should be very strong since surface diffusion of adatoms, which is usually characterized by activation energies of the order of 0.5–0.7 eV, is generally impossible at low temperature (LT) and becomes allowed at some temperature, intermediate between LT and RT.^{18,19} At LT, one therefore expects that the alkali atoms adsorb in a disordered way.¹⁵ The present system constitutes a model case for a two-dimensional disordered system, where the geometry of the adsorbate is weakly dependent on the interaction with the substrate. There should form at the surface-disordered clusters, the geometrical properties of which are determined by percolationlike theories. The phases deposited at low temperature should be out of equilibrium because of the electrostatic repulsion between alkali atoms and because of the absence of surface diffusion. Annealing to RT allows the atoms to diffuse at the surface in order to maximize their

mutual distances and induces an irreversible evolution to an equilibrium configuration. Such irreversibilities have already been observed^{13–16} and have been related to structural changes in the adsorbates using electron-diffraction results.

In the present work, we investigate the metallicity and the degree of disorder of AM adsorbates on the gallium-rich surface of GaAs(001) between 85 K (LT) and RT. We have compared the adsorptions of potassium and sodium for which the magnitudes of the adatom-adatom and adatom-substrate interactions are different. The presence of metallic transport, localized within the surface clusters, is characterized using two transitions thus revealing that, at this temperature, surface diffusion of Na and K atoms becomes possible. The disappearance of the metallicity under annealing occurs at the same temperature as the onset of surface diffusion. We conclude that the metallicity of the adsorbed phase is related to its degree of disorder. Finally, we determine, for both Na and K, the temperature and coverage range of existence of the disordered metallic phases.

II. PRINCIPLES AND EXPERIMENT

The ultrahigh vacuum system has been described before.²⁰ It consists of a chamber with a background pressure in the low 10^{-11} -mbars range. This very low pressure allowed us to limit the spurious effects of surface contamination, since no contaminants were detected using Auger spectroscopy and since the adsorbate electronic properties were found not to change over a period of several hours. We have used UP^+ structures, well-suited for photorefectance experiments, composed of a thin (100 nm) layer of undoped (U) GaAs grown on a highly p -doped (P^+) GaAs(001) underlayer. The structures had been encapsulated by arsenic after molecular-beam epitaxy growth. After introduction into UHV the sample was annealed at increasingly high temperatures, up to 850 K, in order to remove the arsenic overlayer. Such a procedure is known to produce the gallium-rich surface of GaAs(001)-(4×2)/c(8×2),²¹ which we have verified since the reflectance-anisotropy (RA) spectrum, shown below, exhibits an intense negative line at 2.3 eV, which is characteristic of this reconstruction.²² The sample holder, as described elsewhere,²³ allowed us to stabilize the temperature at any value between 85 K and 850 K. It incorporated a liquid-nitrogen cooler and a heating element situated underneath the sample, which guaranteed that the temperature was homogeneous throughout the sample surface. This temperature was determined, within an uncertainty of 10 K, from the position of the zero-order extremum of the photorefectance (PR) spectra using the known temperature dependence of the fundamental gap of GaAs.²⁴ The AM depositions were performed using thoroughly outgassed generators purchased from SAES. The pressure in the chamber during adsorption was always in the 10^{-11} -mbars range. After each adsorption, the AM's were removed by briefly annealing the sample to 850 K.

For the Auger and EELS measurements we have used a VG hemispherical analyzer. Auger spectra were recorded in the derivative mode, with a peak-to-peak modulation amplitude of 3 eV at an incident electron energy of 3 keV. The

shape of the Ga, As, and K *LMM* lines was found to be independent on coverage, and we monitored the peak-to-peak amplitudes of their first derivatives. Analysis of the Na *KLL* line at 990 eV is less straightforward. First, there is a significant overlap between this latter line and the Ga Auger signal. As a result, we subtracted from the measured signal the signal of the clean surface taking into account the attenuation of the main Ga line at 1070 eV induced by Na adsorption. Second, since the shape of the sodium Auger signal is known to be strongly dependent on the metallic character,²⁵ we used for coverage calibration the integrated Auger Na signal, which is weakly dependent on the line shape.

Electron-energy-loss measurements have been performed with an incident beam energy of 200 eV and a total resolution of about 1 eV, which was sufficient to detect collective excitations of the adsorbed alkali atoms under the form of surface and bulk plasmons. The intensity of the plasmon peaks has been evaluated after subtraction of the background.

The PR technique consists in monitoring the change of reflectivity for a probe beam of energy near the fundamental band gap, induced by the modulation of the photovoltage induced by a modulated pump beam.²⁶ The spectra exhibit the well-known Franz-Keldysh oscillations at above-band-gap energies from the positions of which one obtains the surface-barrier value. This value is reduced with respect to its value V_B in the absence of light excitation because of the photovoltage V_S and is given by

$$V_F = V_B - V_S. \quad (1)$$

The photovoltage is known to increase upon sample cooling²⁷ and to be modified by the presence of a surface-metallic phase. Here, for analyzing the data, we have computed the modulus of the complex Fourier transform of the signal in order to determine the surface barrier from the period of the oscillations.²⁸ The uncertainty of the determination of the barrier value, as found from the position of the corresponding peak, is of the order of 50 meV. The system for PR measurements is a standard one. For the probe beam, we have used a quartz halogen lamp and a monochromator, while the light detector was a silicon photodiode. The pump light, generated by a He-Ne laser, was modulated at a very low frequency of 10 Hz. The probe-beam power density was fixed and equal to $1 \mu\text{W}/\text{cm}^2$, whereas the pump power density was of the order of $1 \text{ mW}/\text{cm}^2$. We have verified that the results are weakly sensitive to the pump-power value.

Reflectance anisotropy spectroscopy (RAS) consists in monitoring the dependence as a function of light energy of the quantity $\Delta R/R = (R_{[1\bar{1}0]} - R_{[110]})/R$, which is a measure of the dependence of the reflectivity on the orientation of linearly polarized light along two principal axes of the (001) surface. For the RAS measurements, the excitation source was a xenon lamp and a monochromator, and its linear polarization was modulated at 100 kHz using a quartz modulator. The light reflected from the sample was detected by a photomultiplier tube, the output of which was connected to the input of a lock-in detector. The high-voltage supply of

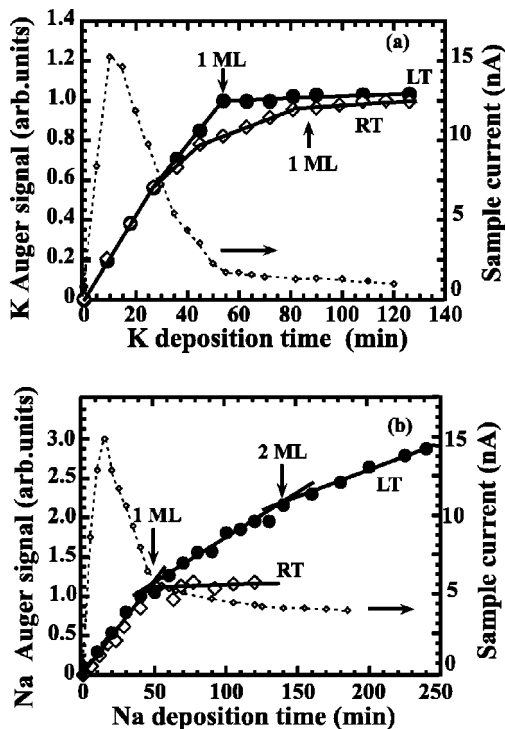


FIG. 1. Dependence of the potassium (a) and sodium (b) Auger-signal intensities on RT and LT adsorption time. For potassium and for RT sodium adsorption, one sees a saturation of the signal, which is our definition of 1-ML coverage. LT sodium adsorption enables to deposit more than 1 ML in a layer-by-layer mode. Also shown in the figures is the change of sample current as a function of adsorption time.

the photomultiplier tube was regulated so that the average signal R was constant over the spectrum. Thus, the output of the lock-in amplifier was simply proportional to the anisotropy signal $\Delta R/R$.

III. DETERMINATION OF THE K AND Na ADSORPTION PROCESSES

For the (110) cleavage face, potassium adsorption has been found to saturate at RT and to proceed in a layer-by-layer mode at LT.¹⁴ For the same orientation, the kinetics of sodium adsorption has, to our knowledge, only been investigated at RT.²⁹ Several breaks in the adsorption kinetics but no clear evidence of saturation have been found. This adsorption has been shown to be reactive at RT, at which intermixing with the substrate has been shown.^{12,29}

For the (001) surface, the processes of K and Na adsorption, to our knowledge, have not been investigated previously. Our results for K are summarized in Fig. 1(a), which shows the peak-to-peak amplitude of the potassium *LMM* line at 252 eV as a function of exposure. For RT adsorption, there is a change of slope at 30-min exposure and the signal eventually saturates at large exposures. In order to distinguish between completion of the first monolayer and the change of sticking coefficient, we have plotted the potassium Auger signal against the signal of the substrate atoms and have observed that the change of slope near 30 min disap-

pears. This allows us to conclude that the change of slope at 30 min is due to a change of sticking coefficient.^{30,31} As is usually performed for this type of interface,³⁰ the coverage at saturation will be taken as a reference for 1 ML.³² For LT potassium adsorption, the signal increases almost linearly up to saturation with a low-coverage behavior, which closely follows the RT changes and saturates at the same level as at RT. Also shown in the figure is the change of the sample current under excitation by the electron beam. This current, which gives the rate of secondary electron emission, exhibits a maximum near a coverage of 0.2–0.3 ML. Such measurement has been shown³¹ to give the same physical information as photocurrent measurements with the advantage of being usable at low AM coverages at which the photocurrent is very small. We conclude that potassium adsorption at the (001)GaAs surface proceeds in a way similar to cesium adsorption at the same surface, and at variance with what has been found for potassium adsorption at the (110) surface.¹⁴ One observes a saturation at a coverage, which is defined as 1 ML and is independent on temperature. Up to 0.6 ML, the sticking coefficient is independent on temperature and for larger coverages it decreases with increasing temperature.

For sodium, our results are shown in Fig. 1(b), which exhibits the dependence of the integrated Na signal as a function of exposure. At RT, the signal saturates at a coverage, which we define as 1 ML, and whereas before saturation, the sticking coefficient is weakly dependent on coverage. In strong contrast, under LT adsorption no saturation is observed. The curve exhibits breaks at 40 min and 130 min, which allows us to exclude three-dimensional growth.^{33,34} The sodium integrated signal at the first break is, within experimental uncertainty, very similar to the saturation level at RT. This indicates that this break is due to completion of the first monolayer, whereas the second break is due to completion of the second monolayer. This interpretation is in agreement with the fact that the LT sample current, also shown in the figure, exhibits a maximum after an exposure of 15 min, which corresponds to a coverage similar to the one found for potassium. We conclude that sodium adsorption at GaAs(001) is strongly dependent on temperature and proceeds in a way similar to potassium adsorption at the (110) surface: At LT, the adsorption proceeds in a layer-by-layer mode with breaks revealing completion of the successive monolayers, whereas at RT adsorption saturates at 1 ML.

Finally, we can rule out the hypothesis of a reactive sodium adsorption at RT, which has been proposed for adsorption on the cleavage face.¹² Indeed, we have monitored the magnitude of the sodium Auger signal as well as of the gallium signal during annealing to RT after LT adsorption of 2 ML of sodium, and have found that these signals stay constant under annealing. This demonstrates that for the (100) surface, annealing to RT does not induce a significant intermixing with the substrate as well as sodium desorption. Even at large coverages, we found that no sodium desorption occurs up to 350 K.

IV. NONMETAL-METAL TRANSITION AS A FUNCTION OF COVERAGE AND TEMPERATURE

A. Formation of a metallic phase under LT adsorption

Figure 2 shows the PR spectra of the clean surface and after selected LT potassium exposures (left panel) as well as

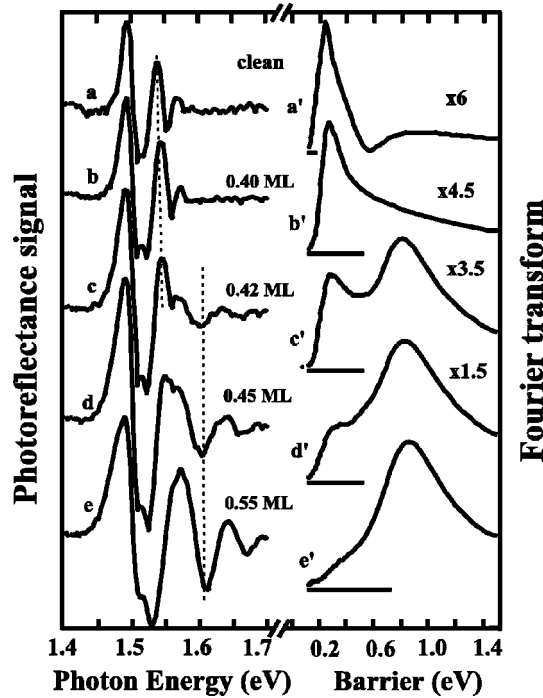


FIG. 2. The left column shows photoreflectance spectra taken for the clean surface and after selected potassium exposures. For each spectrum, the surface barrier is found from a Fourier analysis as shown in the corresponding spectra in the right column. The onset of the nonmetal-metal transition occurs at a coverage of 0.42 ML and is revealed from the abrupt appearance of a second peak in the Fourier spectrum.

their Fourier analysis (right panel). The spectrum of the clean surface, shown in curve *a*, exhibits the well-known Franz-Keldysh oscillations for which the period is related to the surface-barrier value. As found in curve *a'* for the clean surface, the main peak in the Fourier spectrum corresponds to a barrier value of 0.3 eV. In agreement with Eq. (1), the barrier value is smaller at the RT value because of the photovoltage, which is larger at LT.²⁷ After adsorption of 0.4 ML of potassium, the PR spectrum (curve *b*), as well as its Fourier transform (curve *b'*) show only slight changes with respect of the clean surface. Subsequent evaporation of very small amounts of K leads to strong changes of the spectrum shape. After additional adsorption of only 0.02 ML (curve *c*), there appears additional extrema at an energy situated above 1.60 eV. Such modification is revealed most clearly in the Fourier spectrum (curve *c'*), which exhibits, in addition to the above peak at 0.3 eV, an intense peak that corresponds to a barrier value of 0.9 eV. The presence of two peaks indicates that the surface is laterally inhomogeneous and consists of parts characterized by a barrier value of 0.3 eV together with other parts where the barrier is of 0.9 eV. The physical implications of such lateral inhomogeneities will be discussed in Sec. VI. Subsequent adsorption leads to the abrupt decrease of the peak at 0.3 eV so that, in the final stage of this evolution (0.55 ML, curves *e* and *e'*), only the peak at 0.9 eV is observed in the Fourier transform. The changes of surface barrier induced by potassium adsorption at LT are summarized in Fig. 3(a). For each coverage, we have shown

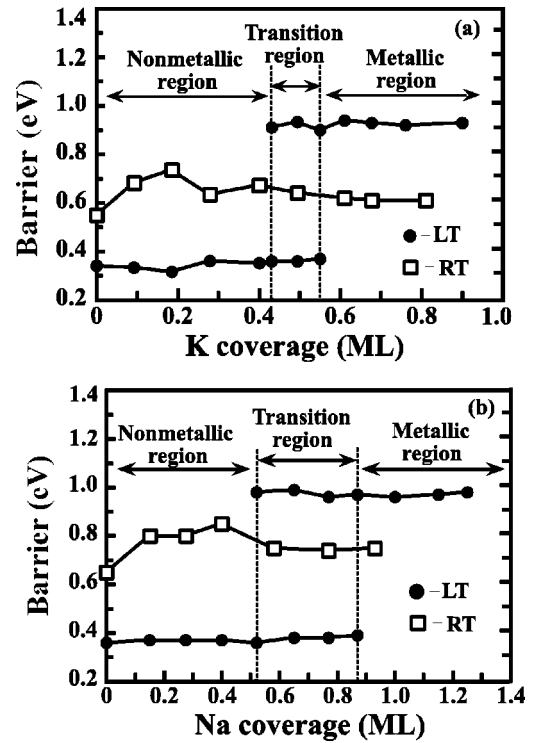


FIG. 3. Surface-barrier changes for K (a) and Na (b) adsorption under LT and RT adsorption.

(black dots) the observed barrier values. At a coverage of 0.42 ML at which a second peak abruptly appears in the Fourier spectrum, we have represented two dots that, respectively, correspond to the two distinct barrier values. We define a transition region as the coverage range where two barrier values are simultaneously observed. This region, delimited by vertical lines in the figure, extends between 0.42 ML and 0.55 ML.

Sodium adsorption at LT induces changes of the PR spectra, which are similar to the ones induced by potassium adsorption. The corresponding surface-barrier changes as a function of coverage, summarized in Fig. 3(b), are qualitatively the same as for potassium adsorption. The final value of the surface barrier is near 1 eV, while the transition region, as revealed by Fourier analysis, is broader than for potassium since it extends between 0.5 ML and 0.9 ML.

Such modifications of the surface barrier can be understood if there occurs a nonmetal-metal transition at the surface. Under formation of a metallic phase, the two terms that appear in Eq. (1) are modified. There is a consensus that the formation of a surface-metallic phase leads to a decrease of the surface photovoltage V_s .^{13,35,36} Such an effect indicates an increase of the surface-recombination velocity and can have several distinct explanations. First, the overlap of the metallic clusters with randomly situated surface defects introduces a new efficient path for surface recombination. Second, the majority-carrier recombination at the surface states becomes easier because of the appearance of a continuum of surface states in the gap region,³⁷ or because the overlap between the hole wave functions and the delocalized metallic states is now strongly enhanced. In Eq. (1), the barrier in the

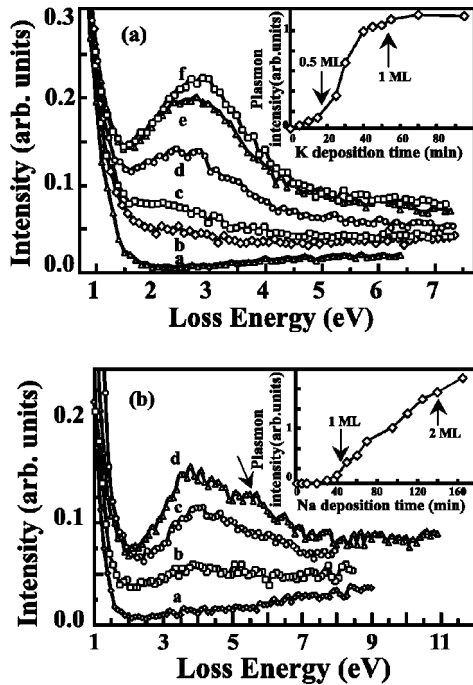


FIG. 4. Electron-energy-loss spectra under adsorption of K (a) and Na (b). For potassium adsorption, the curves, respectively, correspond to the clean surface (a), coverages of 0.3 ML (b), 0.5 ML (c), 0.7 ML (d), 0.8 ML (e), and 1 ML (f). For sodium adsorption, the curves were taken for the clean surface (a), and coverages of, respectively, 1 ML (b), 1.6 ML (c), and 2.2 ML (d). Shown in the inset of the two panels are the changes of the integrated-plasmon signals as a function of adsorption time.

dark V_B is also changed because the surface Fermi level is now pinned by metal-induced gap states at an energy, which is different from that of the nonmetallic states, which pin the Fermi level before the transition.³⁸ Note that in previous studies,³⁹ metallization of alkali adsorbates on Cu at LT was also observed near 0.5 ML.

In order to provide independent proof for the formation metallicity, we have performed EELS investigations of the interface looking for two-dimensional surface plasmons of alkali metals, which are characteristic of a metallic phase.⁴⁰ Figure 4(a) shows the measured loss spectra after several K exposures. The signal is normalized to the intensity of the elastic peak, not shown in the figure. In agreement with previous works,^{37,41} the spectrum of the clean surface (curve *a*) shows a weak increase of the loss signal with increasing loss energy due to the transition between the valence and conduction bands.⁴² After 0.1-ML K deposition, we find that the loss intensity above the gap increases with respect to the clean surface. After deposition of 0.3 ML (curve *b*) the inelastic background is increased, indicating the formation of K-induced surface states in the subgap region and above the gap.¹⁴ At a coverage of 0.5 ML (curve *c*), a weak but detectable peak appears at 2.3 eV. As shown in curves *d* and *e*, additional deposition leads to the increase of the intensity of this peak and to its shift towards higher energy up to the energy of surface plasmons equal to 2.6 eV.^{41,43} This shift is similar to the one of the loss peak II observed by high-

resolution EELS during the metallization of GaAs(110) by K adsorption at LT.¹⁴ As expected, beyond the saturation coverage, the plasmon peak no longer changes (curve *f*). The final plasmon energy is that of two-dimensional surface plasmons with no clear bulk-plasmon signal at 3.7 eV.⁴³ Shown in the inset of Fig. 4(a) is the evolution of the integrated intensity of the plasmon signal as a function of exposure time. The surface-plasmon peak starts to develop at 0.3–0.5 ML, in good agreement with the EELS results on GaAs(110) at LT¹⁴ and with the surface-barrier changes at the (001) surface, shown in Fig. 3(a). These results fully support the occurrence of a nonmetal-metal transition.

For sodium, electron-energy-loss spectroscopy confirms the appearance of a metallic phase. Figure 4(b) shows selected spectra for the clean surface (curve *a*) and for several Na LT exposures. At 0.5 ML, we observe an increase of the inelastic background indicating the formation of Na-induced surface states in the subgap region and above the gap. At 1 ML (curve *b*) there appears a peak at 3.9 eV, which corresponds to the two-dimensional surface-Na-plasmon energy.⁴³ Subsequent deposition leads to further increase of the loss-peak intensity. The shape of the Na-plasmon peak becomes asymmetric and is composed of a surface-plasmon signal near 3.9 eV and of a shoulder at the bulk-plasmon energy (5.7 eV), marked by an arrow in the figure. The bulk plasmon is observed at a coverage larger than approximately 1.5 ML as shown in curves *c* and *d* taken at, respectively, 1.6-ML and 2.2-ML coverages. The present result further confirms the conclusion of the Auger analysis that it is possible to adsorb more than 1 ML at LT.

The inset of Fig. 4(b) shows the dependence of the sum of surface- and bulk-plasmon intensities as a function of Na-deposition time. In agreement with the Auger results, the integrated-plasmon intensity is a linear function of the deposition time of Na and does not saturate, at least up to 2.5 ML. Surface plasmons are observable above a coverage of 0.8–0.9 ML, that is, at a coverage slightly higher than the onset of the surface-barrier change, which occurs 0.5–0.7 ML.

B. RT adsorption

In sharp contrast with the results presented in the preceding subsection, the nonmetal-metal transition is not observed if adsorption is performed at room temperature. Shown in Figs. 3(a) and 3(b) is the coverage dependence of the barrier for, respectively, potassium and sodium adsorption at RT as found using PR spectroscopy. The maximum coverages is 0.9 ML, since beyond this value the PR signal is very weak. For the clean surface, we find a barrier of approximately 0.6 eV, in reasonable agreement with previous results.^{44,45} The most significant barrier changes are obtained for coverages smaller than 0.1 ML. The surface barrier increases by 0.2 eV, in a way similar to what has been reported for cesium adsorption⁴⁴ because the adsorbed AM atoms behave as electron donors, transferring the charge to acceptor states of *p*-type GaAs.^{12,44} No abrupt barrier change is observed under subsequent adsorption and at large coverage the barrier of 0.7 eV, is lower than the LT one by 0.3 eV. If a significant metallic phase was present at the surface, the photovoltage

would be negligible and the Fermi level would be pinned at the same position as at LT. We conclude that, as found from PR spectroscopy, no metallicity develops at RT. In the same conditions, we did not observe two-dimensional (2D) surface plasmons of K and Na during deposition at RT as the measured spectrum only showed an inelastic background. The absence of Cs-plasmon peaks on GaAs(100) surface at RT is also confirmed by EELS investigations.⁴⁶

C. Annealing to RT after LT adsorption: Metal-nonmetal transition

The results presented in the preceding section suggest that the metallic phase created by LT adsorption should be destroyed under anneal to RT. Indeed, if at the end of the LT adsorption, we anneal to RT and perform a subsequent cooling to LT, we observe that the PR spectrum is completely identical with the one obtained after LT adsorption before the onset of the transition (curve *b* of Fig. 2). The barrier is now back to its value of 0.3 eV because a significant photovoltage can build up. On the other hand, Auger spectroscopy shows that in the same conditions, the alkali atom concentration stays constant and that no alkali desorption takes place. This indicates that the destruction of the metallic phase under annealing is irreversible and that this latter phase is metastable.⁴⁷ In order to determine the temperature range in which the metal-nonmetal transition occurs, we have performed a series of annealings to increasing temperatures. After each annealing, the sample was cooled again to LT and the PR spectrum was taken. All the spectra were thus taken in identical conditions of temperature and coverage, and their differences can only be due to irreversible modifications of the electronic properties of the adsorbate caused by structural changes, which occur during annealing. Shown in Fig. 5(a) (full circles) is the barrier change as a function of annealing temperature after LT adsorption of 0.9 ML of potassium. Up to 130 K, the barrier decreases, which shows that some evolution occurs in the adsorbate but that the surface phase is still metallic. In the temperature range situated between 130 K and 200 K, Fourier analysis reveals that, in addition to the peak that corresponds to the metallic phase, there appears a second peak close to 0.3 eV [white dots in Fig. 5(a)], which is characteristic of the nonmetallic phase. This shows that, in the same way as for the appearance of metallicity under LT adsorption, the destruction of this metallicity under anneal exhibits an intermediate regime where both a metallic and a nonmetallic phase coexist. Note that in the present case, the barrier that characterizes the metallic phase continuously decreases, whereas its value under LT adsorption is constant and independent on coverage. After annealing above 210 K, the barrier has recovered its value of 0.3 eV and only one peak is observed in the Fourier spectrum, which proves that the metallic phase has essentially been destroyed by the latter anneal. As expected, a second series of annealing (full squares) does not induce any further barrier change.

The temperature change of the intensity of the surface-plasmon peak during annealing is shown in Fig. 5(b). After an initial intensity decrease up to 125 K, the signal is constant up to 200 K and decreases upon further anneal. The

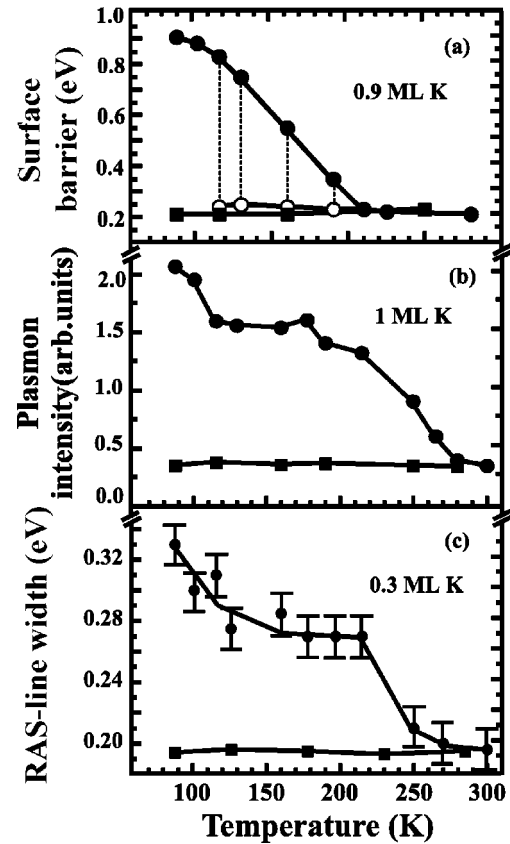


FIG. 5. Effect of annealing following K adsorption at LT. The top panel shows the change of surface barrier (full circles) as a function of annealing temperature, as found from the PR spectrum taken at LT after the anneal. In the intermediate temperature range between 130 K and 200 K, a distinct barrier value is found in the Fourier analysis of the spectrum, (white circles) which reveals the appearance of the nonmetallic phase. The middle panel shows (full circles) the changes of plasmon-signal intensity under anneal as a function of temperature. The bottom panel shows the changes of the width of the line at 2.3 eV of the RA signal (see Fig. 7) after annealing to a given temperature and cooling to LT. In the three panels, full squares show the evolution of the corresponding quantities during a second annealing procedure following the first one.

plasmon peak completely disappears and the final spectrum measured at RT is similar to the spectrum measured at a potassium coverage of 0.3 ML [curve *b* of Fig. 4(a)] as well as to the spectrum observed after adsorption of 1 ML at RT. In the same way as the surface-barrier change, the disappearance of the surface plasmon signal is irreversible. Note that the temperature at which this signal disappears, 270 K, is larger than the temperature of 210 K at which the evolution of the surface barrier is complete.

For sodium, the behavior of surface barrier and plasmon intensity is qualitatively the same as for potassium. As shown in Fig. 6(a), the surface barrier recovers its initial value of 0.3 eV after annealing to 200 K. Figure 6(b) shows that the temperature at which the plasmon peak disappears is 250 K. One significant difference with the case of potassium adsorption is, however, that the surface barrier as well as the plasmon intensity do not decrease at initial stages of anneal-

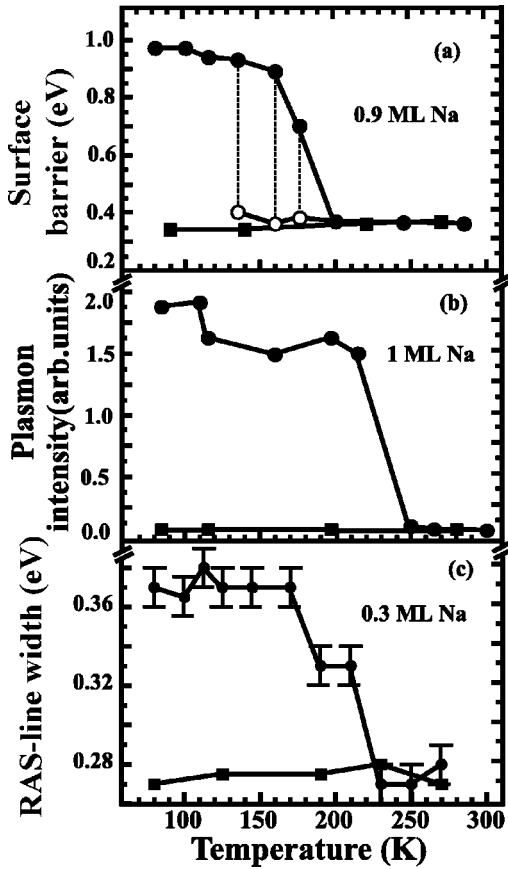


FIG. 6. Same as Fig. 5, effect of annealing after Na adsorption

ing, and that the changes of barrier- and surface-plasmon signal are more abrupt than for potassium.

D. Surface diffusion of alkali atoms and disorder-order transition

In order to interpret the above results, it is necessary to determine the temperature at which surface diffusion of alkali atoms becomes allowed. This is performed in the present section using RAS. Shown in curve *a* of Fig. 7 is the RA spectrum of the clean surface at LT. This spectrum shows a negative signal near 2.3 eV, which is characteristic of the gallium-rich surface reconstruction.⁴⁸ Qualitative information about the order of the adsorbate can be obtained from the observation of the width of this latter signal in the same way as performed before.¹⁸ Shown in curve *b* of Fig. 7 is the RA spectrum obtained at LT after adsorption of 0.3 ML of potassium. The line is shifted to 2.2 eV because potassium adsorption modifies the energy of the levels that participate in the optical transition, and it is significantly broader than the corresponding line for the clean surface. Shown in curve *c* is the spectrum measured at LT after cycling to RT. The overall position of the line at 2.2 eV is unchanged but its width is significantly smaller. These results are the same as the ones observed for cesium adsorption¹⁸ and can be given the same interpretation. The modification of the RA signal is due in the perturbation of the localized electronic states participating in the optical transitions by the adsorbed atoms,

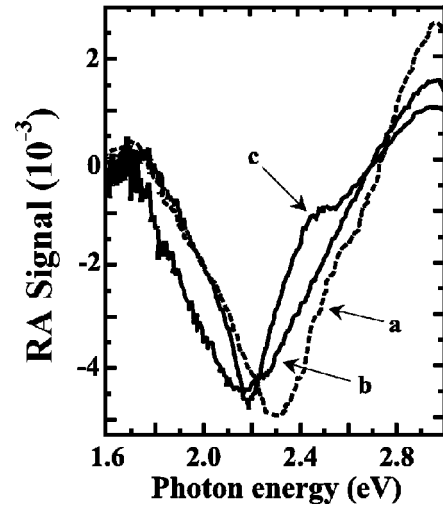


FIG. 7. Curve *a* shows the RA spectrum of the clean surface taken at LT. Curve *b* shows the corresponding spectrum after LT adsorption of 0.3 ML of potassium. Curve *c* shows the spectrum of the same surface after cycling to RT. The fact that this latter curve exhibits a smaller linewidth is a manifestation of the disorder-order transition, which occurs under anneal.

and the broadening induced by LT adsorption is due to the changes of surface-barrier and -plasmon signal intensity shown, respectively, in Figs. 6(a) and 6(b). The disappearance of the sodium metallic phase occurs at a temperature of 220 K, at which surface diffusion becomes allowed. Unlike the case of potassium, the linewidth and the plasmon signal stay constant up to at least 180 K, which shows that little sodium-surface diffusion occurs for temperatures lower than this value and that at LT all the degrees of freedom of the adsorbate are frozen.

The temperature at which surface diffusion takes place is related to the value of the surface-diffusion constant, which is characterized by an activation energy E_d for surface diffusion. Using the same method as published elsewhere¹⁸ we write the diffusion constant D in the form

$$D = D_0 \exp(-E_d/kT) = l^2/\tau, \quad (2)$$

where τ is the duration of the anneal and l is the diffusion length of the order of the dimension of the unit cell. The preexponential factor $D_0 = a_0^2 \tau$ is related to the interatomic distance $a_0 = 0.4$ nm and to a phonon frequency $\nu \approx 10^{13}$ Hz. Taking the temperature at which the linewidth strongly changes under annealing, we find that this activation energy for sodium is of the order of 0.60 eV. For potassium, the dominant activation energy is of the order of 0.70 eV, whereas some sites have an activation energy smaller than 0.4 eV. These values should be compared with the activation energy of 0.7 eV found for diffusion of cesium at the same surface.¹⁸ Note that for potassium diffusion on Ru(001) at 220 K, the activation energy was found to be smaller and equal to 0.35 eV at $\Theta = 0.33$ ML.⁴

E. Phase diagrams

We have shown the following in the preceding sections.

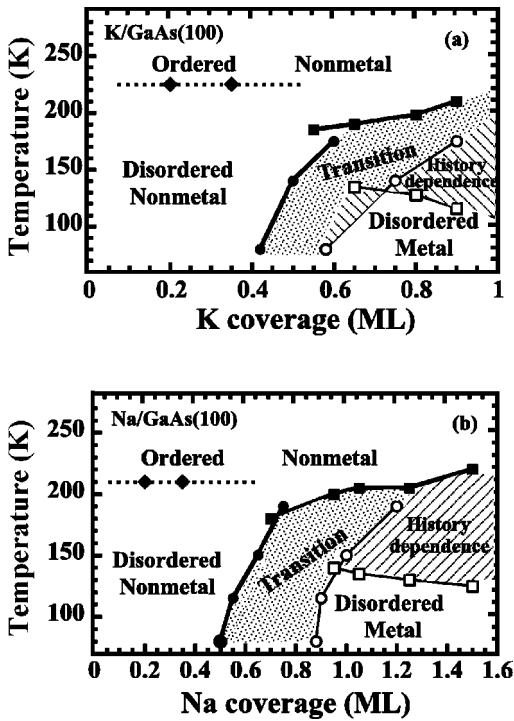


FIG. 8. Phase diagrams of K (a) and Na (b) as a function of coverage and temperature. These diagrams show both the metallicity (as found using PR spectroscopy) and the degree of order. Shown as shaded regions are the zones where a metallic and a nonmetallic region coexist at the surface. Also shown as hatched regions are zones where the electronic-surface properties depend on the history of the preparation procedure.

(i) At a coverage smaller than 0.5 ML and at LT; both for potassium and sodium, the adsorbate is disordered because surface diffusion is not allowed, and is insulating.

(ii) At coverages larger than 0.5 ML at LT, there abruptly appears a metallic phase and there exists an intermediate coverage range in which both metallic and nonmetallic phases are found to coexist. At larger coverage, the insulating phase disappears and only the metallic phase is observed.

(iii) Under annealing to RT, surface diffusion becomes allowed and induces a disorder-order transition. For sodium, this diffusion becomes allowed rather abruptly, whereas for potassium some diffusion already occurs at the initial stages of annealing.

(iv) Upon annealing, there also occurs a converse metal-nonmetal transition at a temperature similar to the one at which ordering takes place at low coverage.

These results are presented in the form of phase diagrams as a function of temperature and coverage, shown in Figs. 8(a) and 8(b) for potassium and sodium, respectively. The full squares show as a function of coverage the temperature of complete disappearance of the metallicity under annealing. The open squares show the onset of the transition region at which one starts to observe a nonmetallic behavior. In order to completely determine the limits of the metallic phase, we have also performed AM depositions at intermediate temperatures. In the same way as for the results presented above, the PR spectra were taken after cooling the

sample to LT after each adsorption process. Fourier analysis of these spectra also revealed the presence of a transition region, where both a metallic phase and an insulating phase coexist at the surface. For each temperature, the onset of the metallicity and the maximum coverage of the transition region are shown by full circles and by open circles, respectively.

The distinction between metallic and transition regions allows us to reveal a fundamental aspect of the adsorbate: We find that, at significant coverages and intermediate temperatures, there exists a region, shown cross hatched in the figure, where the electronic properties depend on the history of the system preparation. If adsorption is performed at intermediate temperature the system is metallic. If, on the other hand, the same AM coverage is adsorbed at LT followed by an anneal to intermediate temperature, the system is partly metallic and partly insulating although the coverage and temperature are the same as in the former case. Such phenomenon has also been observed for AM adsorption on metals⁵ and has been correlated with structural properties. Distinct systems such as spin glasses are also known to exhibit a space of configurations, which consists of many distinct free-energy valleys separated by high mountains, which induces a strong dependence of the system configuration on the history of its preparation.⁴⁹

V. DISCUSSION

Complete interpretation of the above results requires investigation of the geometry of the adsorbate on a microscopic scale as well as calculations of electronic structure and is beyond the scope of the present work. Since experimental investigations⁶ and theoretical analysis⁵⁰ have so far been performed essentially for RT adsorption on the cleavage face; we limit ourselves here to a qualitative discussion.

A. LT adsorption: Nonmetal-metal phase transition in a percolationlike system

The observation of metallicity indicates that there appear at the surface, clusters containing a number of atoms larger than a critical value N_c . For regular 3D clusters, if the atom number is larger than this value, the energy difference between discrete electronic levels, equal to the width W of the AM-induced band divided by the number N of atoms, becomes smaller than kT so that a continuum of states appears. This phenomenon has been called a size-induced nonmetal-metal transition.⁵¹

For potassium adsorption, and for sodium adsorption at submonolayer coverage, the adsorbate consists of two-dimensional clusters. At LT, since surface diffusion of isolated atoms is only allowed at a larger temperature, the alkali atom adsorbs at the site where it impinges at the surface.⁵² As a result, the clusters are disordered and their geometrical properties are described by percolationlike theories.⁵³ In the framework of these theories, the cluster size increases with coverage as a power law, that explains the abrupt appearance of clusters that have a sufficient number of atoms to exhibit metallic properties. Due to this strong dependence of the cluster size on coverage, the coverage at which metallicity

appears should only weakly depend on the chemical nature of the AM, and should be slightly smaller than the percolation threshold (equal to $p_c \sim 0.59$ for site percolation on a square lattice) at which an infinite cluster is formed. The experimental coverage for metallicity is indeed close to p_c and is similar for sodium and potassium.

The fact that the nonmetal-metal transition is discontinuous and the coexistence of two phases near the transition suggests that, in the same way as proposed at the Li/Bi interface,² the transition is of first order. In order to evaluate the cluster size for metallicity near the transition threshold, it is necessary to discuss the experimental techniques in more detail. Here, we use two criteria for metallicity, which are the presence of a peak in the loss spectrum at the known energy of the surface plasmon and the abrupt disappearance of the photovoltage. This disappearance occurs when the metallic clusters overlap randomly situated defects, which introduces an additional efficient path for surface recombination. Such phenomenon occurs when the cluster size is comparable with the average distance between surface defects. Since the density of surface states is of the order of 10^{12} to $5 \times 10^{12} \text{ cm}^{-2}$,⁵⁴ the average distance between these states can be qualitatively estimated as of the order of 5–10 nm. Taking an AM coverage at saturation of $4\text{--}6 \times 10^{14} \text{ cm}^{-2}$ range,³⁰ such clusters should contain approximately 10^2 atoms. This value is probably an upper boundary since there may exist metallic clusters smaller than the distance between defects. The EELS results also give us a lower boundary to the critical cluster size for metallicity, since an amount of 10 atoms is known to be sufficient for surface plasmons to be excited in the cluster.⁵¹ From a theoretical point of view, the number of atoms for metallicity can be estimated from the Mott-Ioffe-Regel criterion, according to which the size-induced nonmetal-metal transition occurs in a 1.5–4-nm region. Thus, in order to observe metallic properties in a 2D cluster, a number of at least 20 atoms is required, which corresponds with the above order of magnitude estimates.

We now discuss the presence of a transition region in which both a metallic and a nonmetallic phase coexist at the surface, and the characteristic dimension of the lateral inhomogeneities. The observation of such lateral photovoltage inhomogeneities implies that the electrical conductivity in the plane of the surface is not sufficient to equilibrate the electric charges between the metallic and nonmetallic patches of the surface. We have verified the validity of such hypothesis by changing the temperature, which should strongly modify the surface conductivity. Shown in curves *a* and *b* of Fig. 9 are the PR spectrum of the clean surface and the same spectrum after deposition of 0.9 ML of potassium at an intermediate temperature of 180 K. The corresponding Fourier spectra are shown in curves *a'* and *b'*. As seen in the phase diagram of Fig. 8(a) using the coverage and temperature values, this case corresponds to the transition region. However, curve *b* only exhibits one peak. The explanation is that, at this increased temperature, the surface conductivity is sufficient to average out the electrical charge at the surface. Subsequent cooling to LT, which is known not to change the system's geometrical properties, strongly modifies the spectrum (curve *c*), and gives rise to the appearance of two dis-

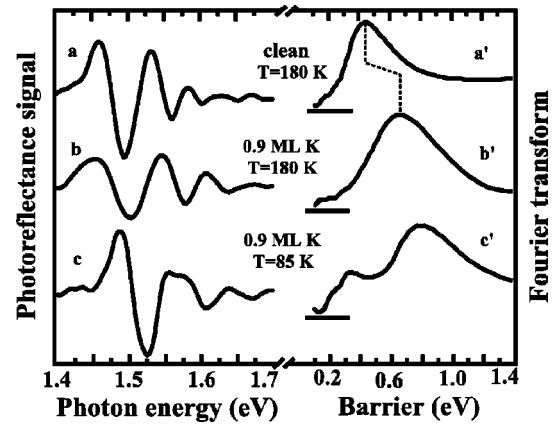


FIG. 9. The left column shows photoreflectance spectra, taken for the clean surface at 180 K (a), after adsorption of 0.9 ML of potassium at 180 K (b) and after subsequent cooling to 85 K (c). For each spectrum, the surface barrier is found from a Fourier analysis, as shown in the corresponding spectra in the right column.

tinct peaks in the Fourier spectrum (curve *c'*). The explanation is that, at LT the surface conductivity is reduced so that lateral charge inhomogeneities can develop at the surface. As found from elementary electrostatics, this implies that the characteristic dimension of the lateral inhomogeneities is comparable with the depth at which the PR signal is observed, which is of the order of a fraction of the space-charge layer. As a result, we conclude that the extension of the lateral inhomogeneities is of the order of 10 nm.

B. Driving force for ordering under annealing to RT

The system under annealing to RT progressively loses its percolation nature as surface diffusion becomes thermodynamically allowed. In order to interpret the evolution of the geometrical and electronic properties of the adsorbate, we distinguish three regimes depending on coverage.

(i) At low coverage, the effect of adatom-adatom repulsion is weak and the observed disorder-order transition is due to diffusion of individual atoms at the surface.¹⁸

(ii) For intermediate coverages larger than the one at which the nonmetal-metal transition is observed, the reorganization of the adsorbate rather occurs because of the repulsive interaction between AM's, in order to minimize the strain energy, and via elementary AM diffusion processes towards unoccupied surface sites. As shown elsewhere using simulations,¹⁶ the larger clusters should be broken into smaller clusters that are likely to be nonmetallic depending on their size and shape.

(iii) If the coverage is near saturation, there are few empty sites at the surface so that surface diffusion cannot occur in the same way. In this regime, it is quite surprising to note that the change under annealing of the surface-plasmon intensity at saturation coverage is in perfect correspondence with the RAS measurements taken at 0.3 ML. Such agreement demonstrates that, at saturation, the elementary evolution steps for disruption of the metallic phase are still diffusion of adsorbed atoms out of the surface potential wells in which they are trapped. The irreversible evolution of the ad-

sorbate may also involve a change of the distance between the adatom and the substrate, in order to maximize the distances between AM's.⁵⁵

The main difference between the structures of the adsorbates at RT and at LT is the difference in the cluster size. At RT, the measured loss spectra at saturation only show an increase of the inelastic background below and above the gap. As already observed at RT in distinct systems,^{37,41} two loss peaks have been found in the subgap region and have been attributed to collective excitations in small 2D clusters, such as the clusters found for GaAs(110) at RT, which contain five Cs atoms or four K atoms.⁶ Note finally that, as shown in Figs. 5 and 6, the disappearance of metallicity under annealing as probed by PR occurs at a temperature lower than the one at which the plasmon signal in the loss spectrum disappears. This is because the decrease of the photovoltage revealed by PR spectroscopy is only observed if there exist clusters larger than the average distance between the surface traps, which are able to efficiently discharge them. Such size is likely to be larger than the actual cluster size for metallicity, as characterized from the observation of surface plasmons in the loss spectrum. The same argument explains that the appearance of metallicity, as found by PR, is more abrupt than as found by EELS.

C. Comparison between Na and K

The main difference between the phase diagrams lies in the larger width of the transition region for sodium. At LT, this width is of 0.35 ML for sodium and of 0.17 ML for potassium. However, one would expect that the Na and the K phase diagrams exhibit more significant differences, since both the alkali-alkali interaction and the alkali-substrate interaction are different. The activation energy for diffusion of individual atoms at the surface, which was estimated using RAS, is a measure of the interaction with the substrate and has been found here to differ for the two atomic species (0.6 eV for sodium and 0.7 eV for potassium). The repulsive adatom-adatom interaction induced by the electrostatic interaction between the AM-induced dipoles or the steric effect is also different between K and Na because of the different amount of charge transfer.

At intermediate temperatures, a possible explanation for the similarity is that the maximum size of the AM clusters is mostly determined by the strain energy of the substrate. This maximum size may be different for potassium and sodium because of the different repulsion between AM's, but the maximum strain energy, which determines the temperature of disruption of the metallic clusters, is similar for the two AM's because it depends mostly on the substrate.

VI. CONCLUSION

We recall the main results of the present work.

(a) We have investigated the adsorption process of potassium and of sodium on GaAs(100) at LT and RT. Whereas LT and RT adsorption of potassium as well as RT adsorption of sodium saturate at a coverage that we define as 1 ML, it is possible to deposit at LT more than 1 ML of sodium.

(b) If adsorption is performed at a temperature lower than approximately 200 K, both potassium and sodium form metallic phases near a coverage of 0.5 ML. These phases are out of equilibrium and are irreversibly destroyed under annealing to RT. We have obtained their diagrams of existence as a function of coverage and temperature. These diagrams include a nonmetallic and a metallic region as well as a transition region where the two phases coexist at the surface. These diagrams are quite similar for Na and K although the alkali-alkali and alkali-substrate interactions are different for the two atoms.

(c) At LT, the adsorbate is disordered, since the activation energy for alkali-atom-surface diffusion is large (0.6 eV for sodium, and 0.7 eV for potassium), so that this diffusion is not possible at LT. For sodium, such diffusion only becomes allowed near 200 K, at which the adsorbate becomes ordered. For potassium, surface diffusion becomes progressively allowed, with some individual motions being allowed at a temperature lower than 150 K, whereas diffusion becomes completely allowed at 230 K.

(d) The evolutions under annealing of the surface barrier and of the plasmon intensity are closely correlated with the onset of surface diffusion, which demonstrates that the onset of surface diffusion is the reason for the destruction of the metallic phase, so that both a metal-nonmetal and a disorder-order transition take place under annealing.

ACKNOWLEDGMENTS

Fruitful discussions with J. F. Gouyet, M. Plapp, V. L. Alperovich, and A. S. Terekhov are gratefully acknowledged. We would like to thank R. Houdré for growing the samples used in the present work. The authors are grateful to H. E. Scheibler for the help in evaluation of photoreflectance spectra by Fourier-transform analysis. This work was performed with financial support from NATO (O.E.T.) and from the Center National de la Recherche Scientifique (D.V.D.). This work was partly supported by the Russian Foundation for Basic Research (Grant Nos. 01-02-17694 and 01-02-16802) and by the Federal program "Surface Atomic Structure" [Grant No. 107-25(00)-P].

¹K. Müller, G. Besold, and K. Heinz, in *Physics and Chemistry of Alkali Metal Adsorption*, edited by H.P. Bonzel, A.M. Bradshaw, and G. Ertl (Elsevier, New York, 1989), pp. 65–90, and references therein.

²G.M. Watson, P.A. Bruhwiler, H.J. Sagner, K.H. Frank, and E.W.

Plummer, *Phys. Rev. B* **20**, 17 678 (1994).

³T. Aruga and Y. Murata, *Prog. Surf. Sci.* **31**, 61 (1989).

⁴E.D. Westre, D.E. Brown, J. Kutzner, and S.M. George, *Surf. Sci.* **294**, 185 (1993).

⁵A. Fedorus and E. Bauer, *Surf. Sci.* **418**, 420 (1998).

- ⁶L.J. Whitman, J.A. Strosio, R.A. Dragoset, and R.J. Celotta, Phys. Rev. Lett. **66**, 1338 (1991); L.J. Whitman, J.A. Strosio, R.A. Dragoset, and R.J. Celotta, in *Atomic and Nanometer Scale Modifications of Materials: Fundamentals and Applications*, edited by P. Avouris (Kluwer Academic, Dordrecht, 1993), p. 25.
- ⁷N.J. DiNardo, T. Maeda Wong, and E.W. Plummer, Phys. Rev. Lett. **65**, 2177 (1990).
- ⁸T. Hashizume, Y. Hasegawa, I. Sumita, and T. Sakurai, Surf. Sci. **246**, 189 (1991); P. Soukiassian, J.A. Kubby, P. Mangat, Z. Hurych, and K.M. Schirm, Phys. Rev. B **46**, 13 471 (1992).
- ⁹Y.-C. Chao, L.S.O. Johansson, C.J. Karlsson, E. Landemark, and R.I.G. Uhrberg, Phys. Rev. B **52**, 2579 (1995).
- ¹⁰K.-D. Lee and J. Chung, Phys. Rev. B **55**, 12 906 (1997).
- ¹¹H.L. Meyerheim, N. Jedrecy, M. Sauvage-Simkin, and R. Pinchaux, Phys. Rev. B **58**, 2118 (1998).
- ¹²M. Prietsch, M. Domke, C. Laubschat, T. Mandel, C. Xue, and G. Kaindl, Z. Phys. B: Condens. Matter **74**, 21 (1989).
- ¹³A. Hamawi, Phys. Rev. B **50**, 10 910 (1994).
- ¹⁴C.A. Ventrice, Jr., and N.J. DiNardo, Phys. Rev. B **47**, 6470 (1993).
- ¹⁵B. Goldstein, Surf. Sci. **47**, 143 (1975).
- ¹⁶D. Paget, B. Kierren, and R. Houdré, J. Vac. Sci. Technol. A **16**, 2350 (1998).
- ¹⁷R. Cao, K. Miyano, I. Lindau, and W.E. Spicer, Phys. Rev. B **39**, 12 655 (1989).
- ¹⁸V.L. Alperovich and D. Paget, Phys. Rev. B **56**, R15 565 (1997).
- ¹⁹R.H. Milne, M. Azim, R. Persaud, and J.A. Venables, Surf. Sci. **336**, 63 (1995).
- ²⁰J. Peretti, H.-J. Drouhin, and D. Paget, Phys. Rev. B **47**, 3603 (1993).
- ²¹W. Chen, M. Dumas, D. Mao, and A. Kahn, J. Vac. Sci. Technol. B **10**, 1886 (1992).
- ²²D. Paget, V.L. Berkovits, and A.O. Gusev, J. Vac. Sci. Technol. A **13**, 2368 (1995).
- ²³H.-J. Drouhin, M. Picard, and D. Paget, Rev. Sci. Instrum. **60**, 1167 (1989).
- ²⁴C.D. Thurmond, J. Electrochem. Soc. **122**, 1133 (1975).
- ²⁵M. Polak and A. Livshits, Appl. Surf. Sci. **10**, 446 (1982).
- ²⁶H. Shen and M. Dutta, J. Appl. Phys. **78**, 2151 (1995), and references therein; F.H. Pollak, in *Photonic Probes of Surfaces*, edited by P. Halevi (Elsevier, Amsterdam, 1995), p. 175, and references therein.
- ²⁷M.H. Hecht, Phys. Rev. B **41**, 7918 (1990).
- ²⁸H.E. Scheibler, V.L. Alperovich, A.S. Jaroshevich, and A.S. Terekhov, Phys. Status Solidi A **152**, 113 (1995).
- ²⁹S. Valeri, M. Loli, and P. Sberveglieri, Surf. Sci. **238**, 63 (1986).
- ³⁰G. Vergara, L.J. Gomez, J. Capmany, and M.T. Montojo, Surf. Sci. **278**, 131 (1992).
- ³¹B. Kierren, and D. Paget, J. Vac. Sci. Technol. A **15**, 2074 (1997).
- ³²For cesium adsorption, the saturation concentration has been estimated as $7.2 \times 10^{14} \text{ cm}^{-2}$ (Ref. 15). For the present case, the microscopic properties of the interfaces have not been investigated and the atomic concentration at saturation is unknown.
- ³³As shown in Ref. 34, identification of these breaks as due to a monolayer completion or a change of sticking coefficient cannot be performed using the analysis of the adsorbate signal as a function of the substrate ones, because Auger electrons of the As, Ga, and Na lines have similar energies so that the transmission coefficients for substrate and adsorbate Auger emission are very close.
- ³⁴C. Argile and G.E. Rhead, Thin Solid Films **152**, 545 (1987).
- ³⁵D.A. Evans, T.P. Chen, Th. Chassé, and K. Horn, Appl. Surf. Sci. **56-58**, 233 (1992); M. Alonso, R. Cimino, and K. Horn, Phys. Rev. Lett. **64**, 1947 (1990).
- ³⁶A.L. Musatov and S.Yu. Smirnov, Phys. Solid State **36**, 4 (1994).
- ³⁷O.E. Tereshchenko, V.L. Alperovich, A.N. Litvinov, and A.S. Terekhov, JETP Lett. **70**, 550 (1999).
- ³⁸W. Mönch, *Semiconductor Surfaces and Interfaces* (Springer, Berlin, 1995).
- ³⁹P. Fouquet and G. Witte, Phys. Rev. Lett. **83**, 360 (1999).
- ⁴⁰A. Liebsch, *Electronic Excitations at Metal Surfaces* (Plenum, New York, 1997).
- ⁴¹U. del Pennino, R. Compano, B. Salvarani, and C. Mariani, Surf. Sci. **409**, 258 (1998).
- ⁴²Due to the total resolution equal to 1 eV, it was not possible to measure the onset of the interband transition at 1.4 eV.
- ⁴³C. Kunz, Z. Phys. **196**, 311 (1966).
- ⁴⁴V.L. Alperovich, A.G. Paulish, and A.S. Terekhov, Phys. Rev. B **50**, 5480 (1994).
- ⁴⁵X. Yin, H.-M. Chen, F.H. Pollak, Y. Chan, P.A. Montano, P.D. Kirchner, G.D. Petit, and J.M. Woodall, J. Vac. Sci. Technol. A **10**, 131 (1992).
- ⁴⁶M. Kamaratos and E. Bauer, J. Appl. Phys. **70**, 7564 (1991).
- ⁴⁷This metastability allows us to discard any interpretation involving a thermally induced change in the surface structure of the substrate, or a decrease of the lattice constant and of the vibrations of the surface atoms.
- ⁴⁸I. Kamiya, D.E. Aspnes, L.T. Florez, and J.P. Harbison, Phys. Rev. B **46**, 15 894 (1992).
- ⁴⁹M. Mézard, G. Parisi, N. Sourias, G. Toulouse, and M. Virasoro, Phys. Rev. Lett. **52**, 1156 (1984).
- ⁵⁰F. Flores, Surf. Rev. Lett. **2**, 513 (1995).
- ⁵¹P.P. Edwards, R.L. Johnston, F. Hensel, C.N.R. Rao, and D.P. Tunstall, Solid State Phys. **52**, 324 (1992).
- ⁵²If the adsorption site is already occupied by an atom, the fact that the sticking coefficient is found to be independent of coverage up to 1 ML (Fig. 1) suggests that the newly deposited atom will diffuse until it finds a vacant adsorption site. Due to this effect, empty sites situated at the boundary of a cluster have a larger probability of being populated than isolated sites, but this should not strongly affect the geometrical properties of the clusters.
- ⁵³D. Stauffer and A. Aharony, *Introduction to Percolation Theory* (Taylor & Francis, London, 1992).
- ⁵⁴M.D. Pashley, K.W. Habernern, R.M. Feenstra, and P.D. Kirchner, Phys. Rev. B **48**, 4612 (1993).
- ⁵⁵J. Derrien and A. D'Avitaya, Surf. Sci. **65**, 668 (1977).